# AN IMPROVED MULTIPYRANOMETER ARRAY FOR THE MEASUREMENT OF DIRECT AND DIFFUSE SOLAR RADIATION

Bryce K. Munger & Jeff S. Haberl, Ph. D., P.E.
Energy Systems Laboratory, Mechanical Engineering
Texas A&M University
College Station, TX

## ABSTRACT

This paper describes an improved multipyranometer array (MPA) for the continuous remote measurement of direct and diffuse solar radiation. The MPA described in this paper is an improvement over previously published MPA studies due to the incorporation of an artificial horizon that prevents reflected ground radiation from striking the tilted sensors. In this paper a description of the NIST-traceable calibration facility is provided and preliminary results are presented that compare the MPA predicted beam to beam measurements from a precision normal incidence pyrheliometer and diffuse measurements from a precision shadow-band pyranometer respectively.

## INTRODUCTION

In the later 1980s several large-scale energy conservation projects were initiated in the United States by utilities and government agencies that incorporated long-term, before-after hourly measurements of energy use, including the Texas Pacific Gas and Electric's ACT$^2$ project (PG&E 1992). In these projects the methods used to calculate the measured energy conservation and retrofit savings varied from empirical regression models to calibrated simulation models. In the case where a calibrated simulation model is used to measure the energy retrofit savings it has been shown recently by Haberl et al. (1993) that the accuracy of calibrated simulation model can improve substantially when the simulation is driven by a weather file containing locally measured weather data versus calibration efforts that are based on Typical Meteorological Year (TMY) or other standard weather tapes. In buildings where solar effects are significant there is an additional improvement in simulation accuracy when locally-measured beam and diffuse solar measurements are incorporated as well.

Until recently, the long-term recording of beam and diffuse solar measurements usually required either the use of very expensive microprocessor-based precision instruments, or worse, precision instruments that needed constant manual adjustment to keep them continuously pointed at the sun. In most cases, it is rare to find accurately measured hourly beam and diffuse solar data that extends over several years and does not contain 10% or more missing data.

Fortunately, several developments have lead to a relatively inexpensive, robust device that promises to be capable of providing long-term beam and diffuse solar measurements -- the multipyranometer array (MPA). The earliest work on an MPA related device for measuring diffuse sky radiation was performed in Finland by M. Hämäläien et al. (1985). Further development on the MPA was performed in several countries including the United States where Perez (1986) presented a method for deriving beam radiation from a series of vertically mounted pyranometer, and in Israel where Faiman et al. (1988) refined the design of the MPA around four model. Further advancements were made on the MPA in the United States by Curtiss (1990; 1992; 1993) who investigated different isotropic and anisotropic diffuse sky models, and devised several novel methods for solving the simultaneous MPA equations including an empirically-based statistical model, and artificial neural networks. Curtiss also made several recommendations for improving MPA measurements, including: (1) corrections for the spectral bias introduced by photovoltaic-based solar sensors, and (2), the use of an artificial horizon to eliminate the ground reflectance term which is unknown. This paper reports on preliminary efforts to develop an improved MPA including: (1) the addition of a practical artificial horizon and, (2) side-by-side testing of the MPA predicted data against data provided by three precision instruments, including a cosine-corrected thermopile-type Precision Spectral Pyranometer (PSP), a Shadow Band Pyranometer (SBP), and a Normal Incidence Pyrheliometer (NIP).

## CURRENT WORK

The facility for testing the MPA is located at a university laboratory in central Texas. The test stand is situated on the south side of the laboratory where the data from the sensors is collected by a data logger which is automatically polled weekly so data can be uploaded into a database[1]. Figure 1 is a photograph of the NIST-traceable test bench which shows the PSP (upper right), SBP, NIP, and MPA (lower left). Uniform black shields have been placed in back of each sensor to block the reflection from the wall directly to the north of the test stand. Figure 2 is a photograph of the MPA including the proposed artificial horizon band. The instrumentation used at the site is listed in Table 1

**Table 1: Instrumentation**

| Mfg. | Instrument | Mfg. Stated Accuracy |
|---|---|---|
| Eppley Labs | Precision Spectral Pyranometer (PSP) | ± 0.5 % from 0-2800 W/ $m^2$ |
| Eppley Labs | Normal Incidence Pyrheliometer (NIP) | ± 0.5 % from 0-2800 W/ $m^2$ |
| Eppley Labs | Shadow Band with Black & White Pyranometer (SBP) | ± 1.0 % from 0-1400 W/ $m^2$ |
| LI-COR | LI-200SA Pyranometer Sensor | ± 3.0 % from 0-3000 W/ $m^2$ |

NOTE:, The NIP, PSP, SBP, and Licors were all calibrated at the respective manufacturer's facilities. The NIP on 2/10/93, the PSP on 10/16/92, the SBP on 2/23/93, and the Licors on 9/15/92.

The MPA consists of four photovoltaic-type sensors arranged so that each sensor sees a different portion of the sky. The arrangement of the sensors in the current MPA is the same as the arrangement used by Curtiss (1990). The MPA that was constructed uses four photovoltaic-type sensors, one sensor mounted horizontally, one 40 degree tilted sensor facing due south, one 40 degree tilted sensor facing 60 degrees east of south, and one 40 degree tilted sensor facing 60 degrees west of south as shown in Figure 2.

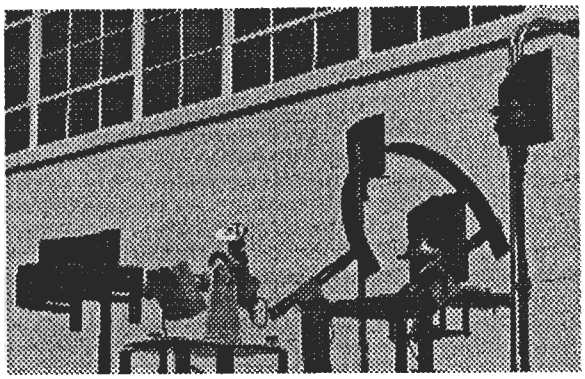

**Figure 1: Test Bench at Energy Systems Lab**

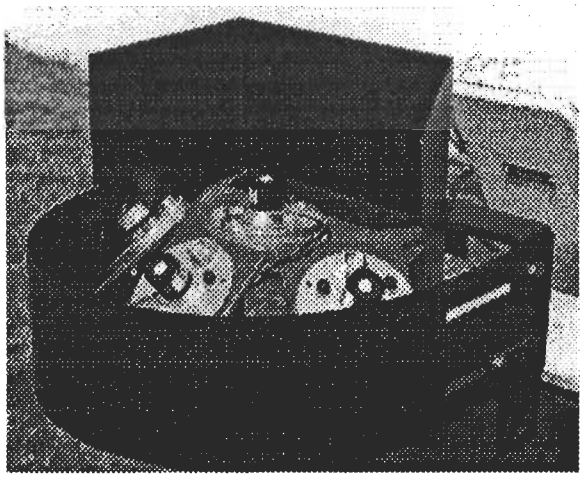

**Figure 2: MPA with Artificial Horizon and Wall Shield**

In order to test the device, the MPA-calculated beam and diffuse measurements were compared with measured data from NIST-traceable sensors capable of continuously measuring global horizontal radiation, diffuse solar radiation and direct-normal beam radiation.

After the initial setup was calibrated and verified the data loggers were set to 15-minute measurement intervals for long-term measurements. Data quality was maintained through a combination of weekly polling and inspection plots (Figures 3 and 4), cross-checking of instrumentation using redundant measurements, and manual daily inspection of the instrumentation alignment.

[1] This data collection effort is part of the LoanSTAR Monitoring program, an eight year $98 million revolving loan program. For additional information on the LoanSTAR program see Claridge et al. (1991)

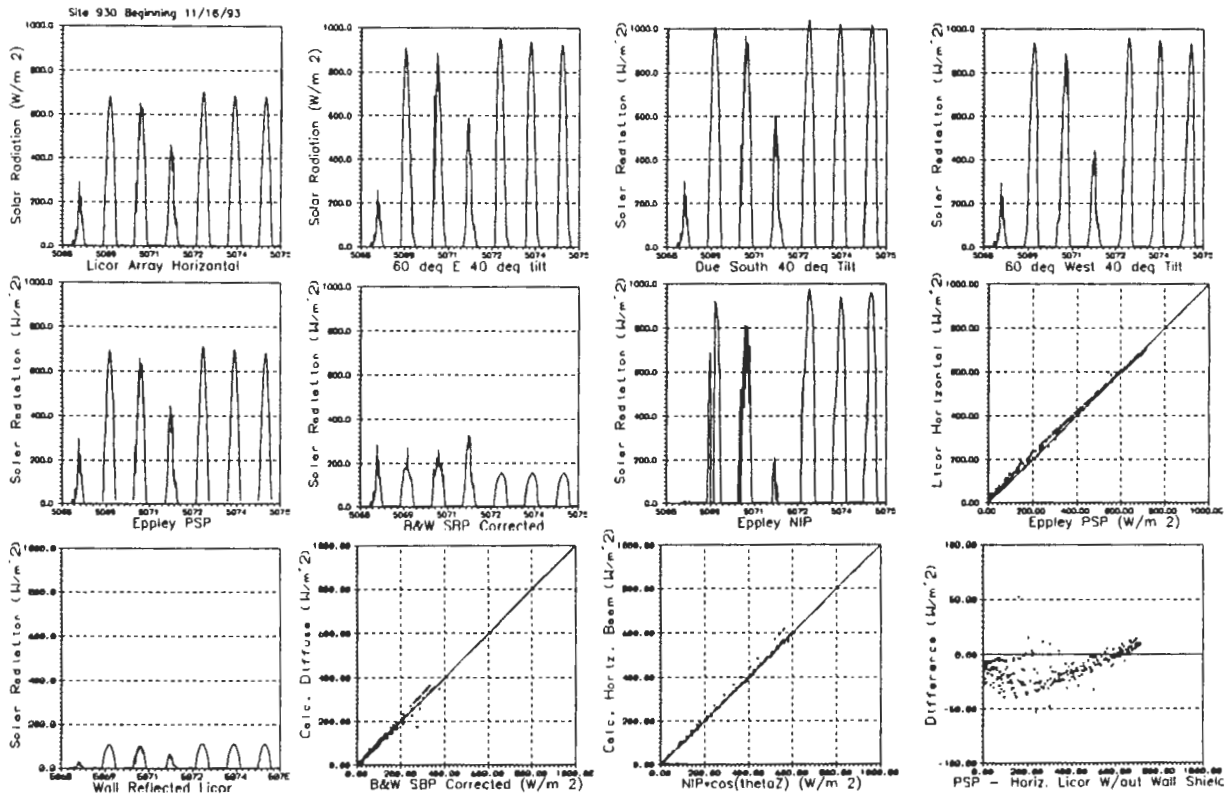


**Figure 3: Inspection plots (page 1)**

The upper row of graphs in Figure 3 present one week of 15 minute data from the MPA sensors beginning with data from the horizontal photovoltaic-type sensor followed by data from the east, west, and south tilted photovoltaic-type sensors. The second row of graphs present data from the PSP, corrected SBP, and NIP precision sensors and a scatter plot that compares the horizontal MPA sensor and the horizontal PSP sensor. The third row shows data from a special shielded horizontal sensor installed to measure only reflected radiation from a nearby white wall directly to the north of the solar test station, followed by three comparative scatter plots. The first scatter plot compares calculated diffuse radiation (i.e., diffuse radiation measured by subtracting the NIP-measured horizontal beam radiation from the global horizontal PSP radiation) to the corrected SBP-measured diffuse radiation[2]. The second scatter plot in the third row compares calculated horizontal beam radiation (i.e., global horizontal PSP-measured radiation minus SBP-measured diffuse radiation) to NIP-measured horizontal beam radiation (i.e., measured direct normal beam radiation times the cosine of the zenith angle). Finally, the last graph displays the difference between the global horizontal solar radiation measured by the horizontal MPA photovoltaic-type sensor to PSP measured global horizontal solar radiation.

In Figure 4 the datasets for each day are plotted to verify the individual daily readings for the week. The dataset is separated by date and the PSP, SBP, NIP, horizontal MPA sensor, and wall reflected measurements are plotted to show the individual response of each sensor. This helps to verify alignment and proper operation of the NIP and SBP, and PSP sensors.

[2]In these preliminary results, the manufacturer's published correction factors were used to adjust the SBP data for the presence of the shading band. In the data shown in Figures 3 and 4 a portion of the NIP data for 11/17/93 is missing due to instrument misalignment.

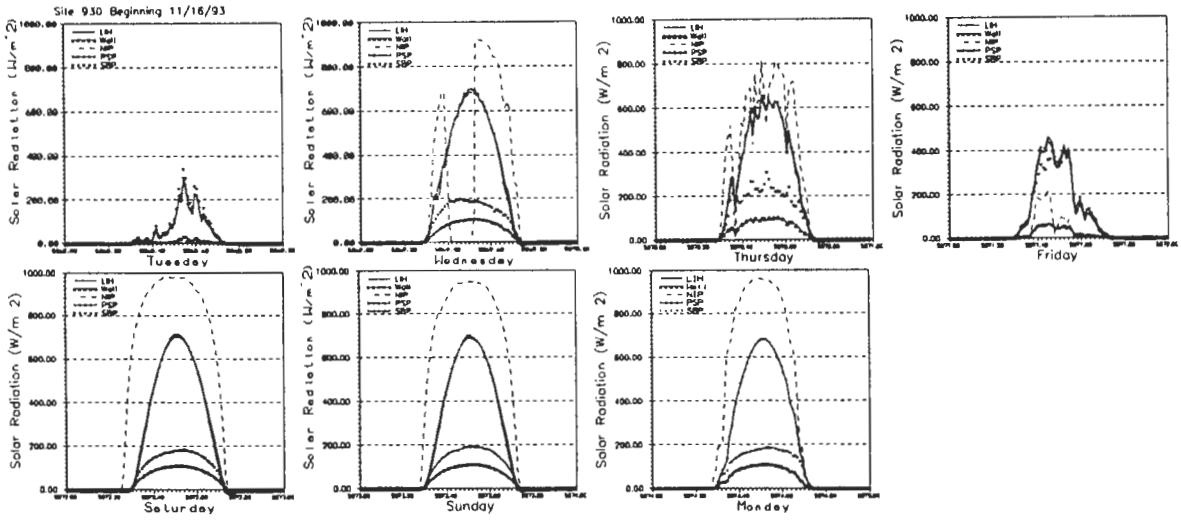


**Figure 4: Inspection plots (page 2)**

## RESULTS

Figures 5 and 6 show the MPA's ability to predict horizontal beam and diffuse radiation. Table 2 shows the CV(RMSE) and RMSE for the different comparisons. Preliminary measurements show that the MPA is capable of predicting horizontal beam radiation to a CV(RMSE) of 10.4% and diffuse radiation to a CV(RMSE) of 11.7% when compared to the NIP and SBP sensors respectively. The use of the Temps-Coulson (1977) anisotropic sky radiation model seems to do an adequate job of computing the diffuse sky characteristics[3].

**Table 2: CV(RMSE), and RMSE Comparison of MPA vs SBP and NIP**

| | SBP Diffuse | NIP Beam |
|---|---|---|
| MPA Diffuse | 0.117<br>11.15 W/ $m^2$ | ---------- |
| MPA Beam | ---------- | 0.104<br>104.43 W/ $m^2$ |
| SBP Diffuse | ---------- | 0.126<br>10.31 W/ $m^2$ |

**Note: SBP Diffuse vs NIP Beam compares the data from the SBP against data from the NIP**

Figures 7 and 8 illustrate one of the remaining sources of error that needs to be addressed, the Differences between the spectral response of the photovoltaic-type sensor and the precision thermopile-type sensor.

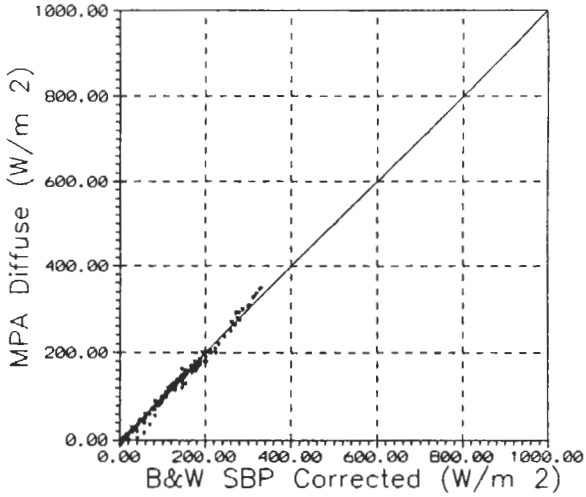


**Figure 5: MPA Diffuse vs Eppley SBP Diffuse**

As shown in Figure 9, a photovoltaic-type sensor responds to radiation in the 0.03 μm to 1.3 μm wavelength range and is less sensitive to radiation outside this range than a thermopile-type precision sensor. The characteristic bias is the reason why the photovoltaic-type sensor over-predicts the solar radiation intensity when the solar radiation falls below 500 W/$m^2$ and under-predicts the solar radiation above 500 W/$m^2$.

[3] An overview of the calculation procedures is included in the appendix.

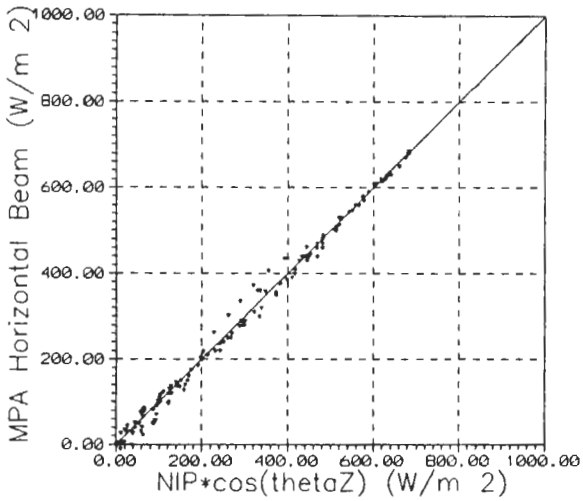


**Figure 6: MPA Horizontal Beam vs NIP Horizontal Beam**

This characteristic is visible in both the unshielded (Figure 7) and shielded data (Figure 8). The shields were placed on the north side of the sensors to block the reflected radiation from the nearby wall. The absence of this under-prediction in the shielded data (Figure 8) tends to indicate that the reflected radiation from the wall directly to the north of the test stand resents a significant portion of the bias, and that the shield partially removes some of the bias. It is speculated that the artificial horizon band provides a similar blocking effect on the ground reflected radiation; hence the improvement in the MPA beam and diffuse predictions.

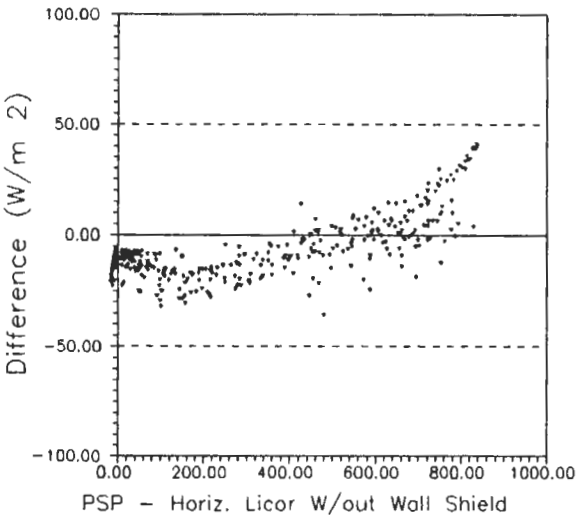


**Figure 7: PSP vs Horizontal Licor Without Shield**

Additional comparisons with and without the artificial horizon should provide a more conclusive analysis. Both the spectral bias and curvature were reported by Curtiss (1990).

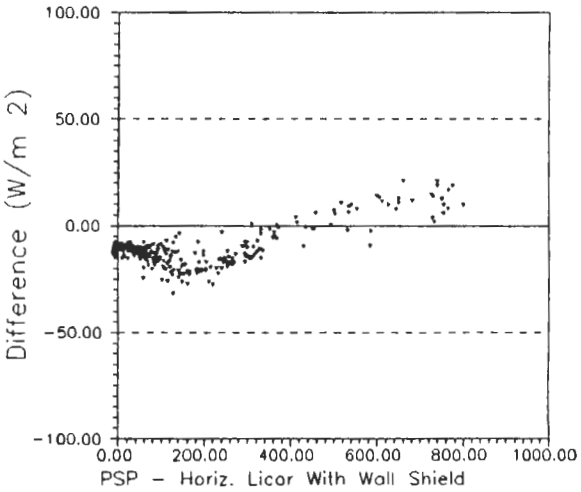


**Figure 8: PSP vs Horizontal Licor With Wall Shield**

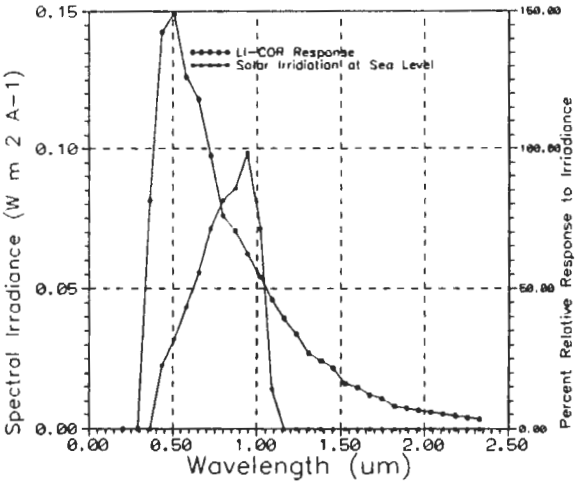


**Figure 9: Relative Spectral Response**
**Source: Licor Manual**

## DISCUSSION

Preliminary measurements have shown that the addition of a simple artificial horizon band to the MPA appears to increase the accuracy of the MPA-predicted beam and diffuse data. The RMSE values received from the MPA calculations are less than the previously reported data without the artificial horizon (Curtiss 1990) which was in the range of 113.1 to 116.4 W/ $m^2$ for a Temps-Coulson (1977) anisotropic sky model. It is felt that the elimination of the unknown ground reflectance contributes to this improvement. Also in this study, the comparison of the MPA beam and diffuse data were made against NIST-traceable solar monitoring equipment located at the test bench, versus NIST-traceable equipment located some distance away as

reported by Curtiss (1990). Most likely, this also contributes to the improved results.

The artificial horizon band addition to the MPA promises to be an addition which will improve the use of the MPA. The artificial horizon developed in this study is specifically designed to be robust enough to be applicable to an MPA in any situation. Additional measurements are underway to refine the comparisons, improve the MPA instrumentation, and develop a spectral correction factor.

## ACKNOWLEDGMENTS

Support by the State of Texas Energy Conservation Office through the LoanSTAR program is gratefully acknowledged. Special thanks for to the following people at the Energy Systems Lab for their assistance on this project: Dan Turner, Chuck Bohmer, Frank Scott, Pat Tollefson, Kelly Milligan, Robert Sparks, Ron Chambers, and John Bryant. Communications with Jan Kreider and Peter Curtiss at the University of Colorado, and Jeff Gordon at Ben Gurion University of the Negev were also extremely useful. The idea for a horizontal shading band was motivated by the Kipp & Zonen display at the 1993 ASME conference.

## REFERENCES

Claridge, D., Haberl, J. O'Neal, D., Heffington, W., Turner, D., Tombari, C., Roberts, M., Jaeger, S., 1991. "Improved Energy Conservation Retrofits with Measured Savings," ASHRAE Journal (August)

Curtiss, P. 1990. "An Analysis of Methods for Deriving the Constituent Insolation Components from Multipyranometer Array Measurements," Masters Thesis, Joint Center for Energy Management. (February).

Curtiss, P. 1992. "An Analysis of Methods for Deriving the Constituent Insolation Components from Multipyranometer Array Measurements," Proceedings of the 1992 ASES/JSEE/KSES Solar Energy Engineering Conference, Maui, Hawaii, pp. 109-117

Curtiss, P. 1993, "An Analysis of Methods for Deriving the Constituent Insolation Components from Multipyranometer Array Measurements," Journal of Solar Energy Engineering, Vol. 115, pp. 11-21.

Duffie, J. A. and Beckman, W. A., Solar Engineering of Thermal Processes, Wiley-Interscience, Madison, Wisconsin, 1991

Diamond, R., Piette, M. Nordman, O., and Harris, J., "The Performance of the Energy Edge Buildings: Energy Use and Savings," Proceedings of the 1992 7th ACEEE Summer Study on Energy Efficient Buildings.

Faiman, D., Zemel, A., and Zangvil, A. 1988. "A method for monitoring Insolation in Remote Regions," Solar Energy, Vol. 39, pp. 327-333.

Haberl, J., Bronson, J., Bou-Saada, T., and O'Neal, D., "A Report on the Impact of Using Measured Weather Data Versus TMY Weather Data in a DOE-2 Simulation of an Existing Building in Central Texas" Energy Systems Laboratory Technical Report, ESL-TR-93/09-2, September, 1993

Hämäläien, M., Nurkkanen, P., and Salen, T., 1985. "A Multisensor Pyranometer for determination of the Direct Component and Angular Distribution of Solar Radiation," Solar Energy, Vol. 35, pp. 511-525.

Koran, W., Kaplan, M. and Steele, T. "DOE-2.1C Model Calibration With Short-Term Tests versus Calibration With Long-Term Monitored Data," Proceedings of the 1992 7th ACEEE Summer Study on Energy Efficient Buildings.

Perez, R., Seals, R., and Stewart, R. 1986. "On Estimating Beam Irridiance from Vertically Mounted Sensors" Proceedings of the 1986 Annual ASES Meeting, Boulder, Co, pp. 180-183.

Temps, R., and Coulson, J. 1977. "Solar Radiation Incident Upon Slopes of Different Orientations," Solar Energy, Vol. 19, pp. 179-184.

## APPENDIX
## Nomenclature

$I_{T,h}$ = Total radiation measured on the horizontal (W/ $m^2$)
$I_{T,se}$ = Total radiation measured on the east of south facing tilted surface (W/ $m^2$)
$I_{T,s}$ = Total radiation measured on the south facing tilted surface (W/ $m^2$)
$I_{T,sw}$ = Total radiation measured on the west of south facing tilted surface (W/ $m^2$)
$I_{b,n}$ = Normal beam radiation (W/ $m^2$)
$I_{d,h}$ = Diffuse radiation measured on the horizontal (W/ $m^2$)
$R_{b,h}$ = Beam coefficient for horizontal
$R_{b,se}$= Beam coefficient for east of south
$R_{b,s}$= Beam coefficient for south
$R_{b,sw}$= Beam coefficient for west of south
$R_{d,h}$= Diffuse coefficient for horizontal
$R_{d,se}$= Diffuse coefficient for east of south
$R_{d,s}$= Diffuse coefficient for south
$R_{d,sw}$= Diffuse coefficient for west of south
$\theta_i$ = Incidence angle of beam radiation
n = day of year
$\beta$ = collector tilt angle
$\phi$ = latitude
$\gamma$ = off-south azimuth angle
$\rho_g$ = foreground reflectance
dec = decimal date
$R_r$ = Reflected radiation coefficient (for the south east sensor)

$$R_{r,se} = \frac{1-\cos(\beta_{se})}{2}$$

$\omega$ = hour angle

$$\omega = \left(dec - (int(dec) + 0.5)\right) * 24 * 15$$

$\delta$= declination = $23.45 \times \sin\left(360 * \frac{284+n}{365}\right)$

### MPA Calculation

The equations for the total solar radiation incident upon the MPA sensors are:

$$I_{T,h} = I_{b,n} * R_{b,h} + I_{d,h} * R_{d,h} \quad (1)$$

$$I_{T,se} = I_{b,n} * R_{b,se} + I_{d,h} * R_{d,se} + I_{T,h}\rho_g R_{r,se} \quad (2)$$

$$I_{T,s} = I_{b,n} * R_{b,s} + I_{d,h} * R_{d,s} + I_{T,h}\rho_g R_{r,s} \quad (3)$$

$$I_{T,sw} = I_{b,n} * R_{b,sw} + I_{d,h} * R_{d,sw} + I_{T,h}\rho_g R_{r,sw} \quad (4)$$

Where the beam coefficient for the horizontal sensor is:

$$R_{b,h} = \cos(\theta_{i,h}) \quad (5)$$

And, the diffuse coefficient for the horizontal sensor based upon the Temps / Coulson (1977) model is:

$$R_{d,h} = \frac{1+\cos(\beta,h)}{2} * \left[1+\sin^3\left(\frac{\beta,h}{2}\right)\right] * \left[1+\cos^2\left(\theta_{i,h} * \sin^3(\theta_z)\right)\right] \quad (6)$$

The incidence angle ($\theta_{i,h}$) for the horizontal sensor is determined from the following:

$$\cos(\theta_{i,h}) = \sin(\delta)\sin(\phi)\cos(\beta,h) - \sin(\delta)\cos(\phi)\sin(\beta,h)\cos(\gamma,h) + \cos(\delta)\cos(\phi)\cos(\beta,h)\cos(\omega) + \cos(\delta)\sin(\phi)\sin(\beta,h)\cos(\gamma,h)\cos(\omega) + \cos(\delta)\sin(\beta,h)\sin(\gamma,h)\sin(\omega) \quad (7)$$

Similar expression are used for the southeast, south and southwest tilted sensors. Without the artificial horizon, these four equations are solved for $I_{b,n}$, $I_{d,h}$, and $\rho_g$. With the artificial horizon these four equations are solved for $I_{b,n}$ and $I_{d,h}$.



Proceedings of the Ninth Symposium on Improving Building Systems in Hot and Humid Climates, Arlington, TX, May 19-20, 1994